Cancer Research

Synergistic Activity of Sorafenib and Sulforaphane Abolishes Pancreatic Cancer Stem Cell Characteristics

Vanessa Rausch[1,3], Li Liu[1,3], Georgios Kallifatidis[1,3], Bernd Baumann[5], Jürgen Mattern[1,3], Jury Gladkich[1,3], Thomas Wirth[5], Peter Schemmer[3], Markus W. Büchler[3], Margot Zöller[2,3], Alexei V. Salnikov[1,4], and Ingrid Herr[1,3]

Abstract

Recent evidence suggests that pancreatic cancer and other solid tumors contain a subset of tumorigenic cells capable of extensive self-renewal that contribute to metastasis and treatment resistance. Sorafenib (SO) is a promising new multikinase inhibitor for treatment of advanced kidney and liver cancers. We report here targeting of pancreatic cancer stem cells (CSC) by SO and the development of a strategy to enhance this effect. Although SO administration diminished clonogenicity, spheroid formation, aldehyde dehydrogenase 1 (ALDH1) activity, growth on immunodeficient mice, proliferation, and angiogenesis and induced apoptosis, we observed SO-induced activation of NF-κB associated with survival and regrowth of spheroids. For enhanced elimination of CSC characteristics by SO, we cotreated cells with sulforaphane (SF). This broccoli isothiocyanate was recently described to eliminate pancreatic CSCs by downregulation of NF-κB activity without inducing toxic side effects. On combination treatment, SF completely eradicated SO-induced NF-κB binding, which was associated with abrogated clonogenicity, spheroid formation, ALDH1 activity, migratory capacity, and induction of apoptosis. *In vivo*, combination therapy reduced the tumor size in a synergistic manner. This was due to induction of apoptosis, inhibition of proliferation and angiogenesis, and downregulation of SO-induced expression of proteins involved in epithelial-mesenchymal transition. Our data suggest that SF may be suited to increase targeting of CSCs by SO. *Cancer Res; 70(12); 5004–13. ©2010 AACR.*

Introduction

Pancreatic cancer is an aggressive malignancy characterized by an extensive local invasion, early systemic dissemination, and pronounced resistance to chemotherapy and radiotherapy (1). Increasing evidence indicates that human pancreatic cancer is driven by "tumor-initiating cells" popularly also known as "cancer stem cells" (CSC) that may contribute to tumor metastasis and therapeutic resistance (2–5). We have recently shown that a $CD24^-/CD44^+$ phenotype characterizes the aldehyde dehydrogenase 1 (ALDH1)–positive, therapy-resistant, spheroid, and colony-forming population in MIA-PaCa2, AsPC1, Capan-1, and BxPc-3 pancreatic cancer cell lines (6). Importantly, conventional chemotherapy or radiotherapy does not completely eradicate CSCs in pancreatic cancer (7, 8), suggesting the need for novel therapies based on the elimination of CSCs.

Sorafenib (SO), a novel multikinase inhibitor, also known as BAY 43-9006 or Nexavar, has shown promising antitumor activity in several clinical phase I/II combination studies with oxaliplatin (9), 5-fluorouracil and leucovorin (10), gemcitabine (11), doxorubicin (12), docetaxel (13), and paclitaxel plus carboplatin (14). Multiple phase I, II, and III trials with SO alone or in combination with other chemotherapeutic drugs are ongoing. Mechanistically, SO inhibits vascular endothelial growth factor (VEGF) receptor-2 and VEGF receptor-3 expressed by endothelial cells and $CD133^+$ circulating hematopoietic progenitor cells (15) and platelet-derived growth factor receptor-β, FLT3, Ret, and c-Kit expressed by vasculature-associated cells and tumor cells (16, 17). These kinases are involved in tumor angiogenesis, as well as in growth and progression of a variety of tumor types such as leukemias and renal cell and hepatocellular carcinomas, suggesting CSC targeting by SO. However, recent studies in mouse models of pancreatic neuroendocrine tumors, glioblastoma, and breast cancer showed an unwanted side effect of SO and related antiangiogenic substances: After initial antitumor activity, enhanced tumor progression and increased metastasis occurred (18, 19). The underlying mechanism may be due to induction of hypoxia by antiangiogenic treatment and selection of highly resistant CSCs adapted to depletion of oxygen and nutrition. Therefore, combination of SO with a "sensitizer" may be necessary for complete elimination of CSCs. A

Authors' Affiliations: [1]Molecular OncoSurgery and [2]Tumor Cell Biology, University of Heidelberg and German Cancer Research Center; [3]Department of General Surgery, University of Heidelberg; [4]Translational Immunology Unit, German Cancer Research Center, Heidelberg, Germany; and [5]Institute of Physiological Chemistry, University of Ulm, Ulm, Germany

Note: Supplementary data for this article are available at Cancer Research Online (http://cancerres.aacrjournals.org/).

Corresponding Author: Ingrid Herr, Experimental Medicine, University Hospital of Heidelberg, Experimental Surgery, Im Neuenheimer Feld 365, 69120 Heidelberg, Germany. Phone: 49-6221-56-5147; Fax: 11-49-6221-56-6119; E-mail: i.herr@dkfz.de.

doi: 10.1158/0008-5472.CAN-10-0066

promising candidate for combination is the dietary food component sulforaphane (SF). This isothiocyanate is enriched in the plant family of *Brassicaceae* and present in high concentration in broccoli. SF inhibits phase 1 cytochrome P450 enzymes, induces phase 2 metabolic enzymes, and acts as an antioxidant by increasing reduced glutathione levels as well as inducing cell cycle arrest and apoptosis. In addition, SF exhibits anti-inflammatory properties and inhibits angiogenesis (20). SF has recently been shown to sensitize pancreatic CSCs by downregulation of NF-κB along with inhibition of CSC properties (e.g., ALDH1 and self-renewal activity, apoptosis resistance, and growth in immunodeficient mice; ref. 6).

In the present study, we used *in vitro* assays and *in vivo* xenograft models to examine the effects of SO on the pancreatic CSC population. We showed that CSCs are diminished by SO, although some clones acquire resistance. This may be due to the observed strong induction of NF-κB signaling by SO. Therefore, we used SF cotreatment, which completely downregulated NF-κB activity and strongly increased the anti-CSC properties of SO.

Materials and Methods

Human primary and established cell lines

BxPc-3 (CSC^{low}) and MIA-PaCa2 (CSC^{high}) pancreatic cancer cell lines were obtained from the American Type Culture Collection and authenticated throughout the culture by the typical morphology. Mycoplasma-negative cultures were ensured by weekly tests. Primary skin fibroblasts were kindly provided by Dr. H-J. Stark (DKFZ, Heidelberg, Germany). Cells were cultured in DMEM (PAA) supplemented with 10% heat-inactivated FCS (Sigma) and 25 mmol/L HEPES (PAA). Human mesenchymal stem/stromal cells were isolated from bone marrow and cultured as described (21).

Reagents

Sorafenib tosylate [*N*-(3-trifluoromethyl-4-chlorophenyl)-*N*′-(4(2-methylcarbamoyl pyridin-4-yl)oxyphenyl) urea] was kindly provided by Bayer Corporation (West Haven, CT) and dissolved in DMSO (Sigma-Aldrich) to a 100 mmol/L stock. This stock was further diluted for *in vivo* studies in a Cremophor EL/100% ethanol mixture (1:1 ratio) to a 4× stock. Sulforaphane [1-isothiocyanato-4-(methylsulfinyl)-butane] (Sigma Aldrich) was dissolved in 100% ethanol to a stock solution of 100 mmol/L. For *in vivo* studies, this stock was further diluted with sterile PBS. A 40 mmol/L Z-VAD-FMK stock (Promega) was prepared in DMSO. The concentration of DMSO in the working solutions did not exceed 0.1% (v/v).

Xenograft tumor models

MIA-PaCa2 tumor cells (2×10^7 in 200 μL of PBS) were injected s.c. into the left and right flanks of 4-week-old NMRI (nu/nu) female mice. Two weeks later, xenografts were minced and subtransplanted into 6-week-old mice. After the tumors had reached a mean diameter of 8 to 10 mm, mice were randomized to six groups of six animals per group. The mice were treated i.p. on 3 consecutive days with SF at a dose of 3 mg/kg or with SO at doses of 30, 40, and 60 mg/kg or with a combination of SF (3 mg/kg) and SO (60 mg/kg). The control group received a Cremophor EL/95% ethanol/PBS mixture (1:1:6 ratio). Tumor growth was monitored as described recently (6). Animal experiments have been carried out at the animal facility of the University of Heidelberg after approval by the Baden Württemberg animal oversight committee (Regierungspräsidium Karlsruhe, Germany).

Measurement of apoptosis

Cells were stained with Nicoletti buffer as described (22) and DNA fragmentation was identified by flow cytometry (FACScan, BD Biosciences).

Viability assay

Viability was measured using MTT as described previously.

Spheroid formation assay

Tumor cells were cultured in human NeuroCult NS-A basal serum-free medium with supplements (StemCell Technologies, Inc.) and spheroid formation was evaluated as described (6).

Colony formation assay

Tumor cells were seeded at a density of 3×10^5 per well in six-well tissue culture plates (BD Falcon). Twenty-four hours later, the cultures were pretreated with SF for 24 hours and subsequently treated with SO for 48 hours. Afterward, cells were trypsinized, washed with PBS, and resuspended in cell culture medium at a density of 200 per well in six-well tissue culture plates and colony formation was evaluated as described (23).

Scratch assay

MIA-PaCa2 cells (6×10^5) were seeded in six-well plates and grown to confluence. Twenty-four hours after treatment, a line was scraped within confluent cells using the fine end of a 10-μL pipette tip (time 0).

Detection of ALDH1 activity

ALDEFLUOR substrate (5 μL; Aldagen, Inc.) was added to 1×10^6 treated tumor cells in 500 μL of assay buffer and incubated for 60 minutes at 37°C. Pretreatment with the ALDH1 inhibitor diethylaminobenzaldehyde was used as a negative control.

Detection of caspase activity

Kits providing fluorochrome inhibitors of caspases (FLICA) were used according to the manufacturer's recommendations (Immunochemistry Technologies) and caspase activity was analyzed by flow cytometry or immunofluorescence microscopy as described (6).

Protein isolation and Western blot analysis

Cell proteins were isolated and Western blot analysis was done as described recently (6).

Electrophoretic mobility shift assay

Whole-cell extract was harvested as described recently (24) and electrophoretic mobility shift assay (EMSA) was done as described (6).

Immunohistochemistry and immunocytochemistry

Immunohistochemistry on 6-μm frozen or paraffin-embedded tissue sections was done as described previously (6). Antibodies used were rat anti-mouse CD31 monoclonal antibody (mAb; PharMingen) and rabbit polyclonal antibodies against cleaved fragment of activated human caspase-3 (R&D Systems), human Ki-67 (Thermo Scientific), and human ZEB1 (Santa Cruz). Mouse mAbs were anti-human Twist2, anti-vimentin (Abcam), and anti–HIF-1α (BD Biosciences).

Statistical analyses

For MTT and fluorescence-activated cell sorting (FACS) measurements, data are presented as the mean ± SD. Data were analyzed using Student's *t* test for statistical significance. $P < 0.05$ was considered statistically significant. For xenografts of nude mice, a distribution free test for tumor growth curve analyses for therapy experiments was used as described by Koziol and colleagues and Kallifatidis and colleagues (25, 26).

Results

SO reduces CSC properties

We used MIA-PaCa2 and BxPc-3 pancreatic cancer cell lines, which we have recently characterized as CSC^{high} and CSC^{low}, respectively (Supplementary Table S1). Morphologically, CSC^{low} cells consist of only one adherent cell phenotype, whereas CSC^{high} cells contain adherent cells and spheroidal floating cells (Fig. 1A). To investigate whether SO targets pancreatic CSCs, both cell lines were treated with 2, 5, 10, 20, or 50 μmol/L SO, and 48 hours later, cell viability was analyzed by MTT assay. SO treatment resulted in a dose-dependent inhibition of viability in both cell lines (Supplementary Fig. S1A). However, SO at the highest concentration of 50 μmol/L was toxic to nonmalignant primary human skin fibroblasts and bone marrow–derived mesenchymal stem/stromal cells (Supplementary Fig. S1B and C). Therefore, SO was applied at a subtoxic concentration of 20 μmol/L in all further experiments. This concentration significantly reduced colony and spheroid formation (Fig. 1B, compare Fig. 3C). However, some small colonies survived, resulting in regrowth of spheroids 30 days later (Fig. 1C). These data indicate that SO alone does not completely diminish the clonogenicity and self-renewal capacity of CSCs *in vitro*.

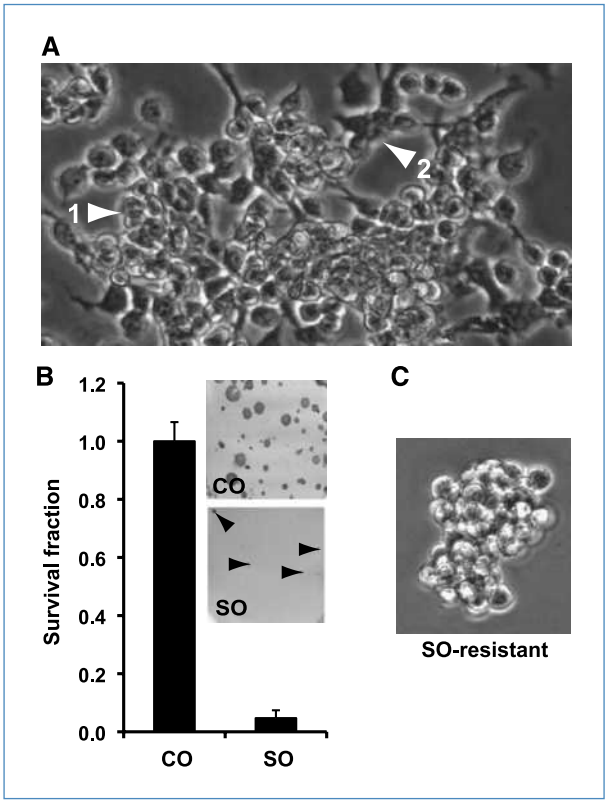

Figure 1. SO reduces cell viability and colony and spheroid formation, but long-term treatment selects resistant CSCs. A, representative image of CSC^{high} MIA-PaCa2 cells (arrow 1, spheroidal floating; arrow 2, adherent). B, CSC^{high} cells were treated with 20 μmol/L SO and colony formation assay was done as described; the survival fraction (% of control = 100%) is shown. C, spheroid formation of CSC^{high} MIA-PaCa2 cells after long-term SO treatment (20 μmol/L, 30 d) is shown under 100× magnification.

SO diminishes the growth of CSCs *in vivo* by inhibition of proliferation and angiogenesis

To investigate the effects of SO *in vivo*, MIA-PaCa2 CSC^{high} cells were s.c. transplanted into nude mice. Treatment with SO at days 11, 12, and 13 after tumor inoculation strongly inhibited tumor growth in a dose-dependent manner (Fig. 2A). No toxic side effects of SO occurred as concluded from the unchanged general condition of mice and constant body weight during treatment (Fig. 2B and data not shown). In xenograft tissue, obtained 17 days after treatment, SO reduced the percentage of Ki-67–positive tumor cells in a dose-dependent manner, suggesting inhibition of proliferation (Fig. 2C and D). Likewise, blood vessel density was decreased by SO as examined by CD31 staining of endothelial cells. Accordingly, apoptosis was induced as concluded from enhanced activity of caspase-3, which was, however, not significant. These data show that SO retards the growth of pancreatic CSC^{high} xenografts by diminishing angiogenesis and proliferation and, most likely, by induction of apoptosis. However, SO did not completely eradicate the tumor mass, suggesting the need for combination therapy to increase the effect.

SO and SF synergistically inhibit CSC characteristics *in vitro*

For sensitization, we pretreated BxPc-3 CSC^{high} and MIA-PaCa2 CSC^{low} cells with SF for 24 hours followed by incubation with SO for an additional 48 hours. This resulted in a more pronounced induction of cell death compared with each substance alone as indicated by cell morphology (Fig. 3A), colony and spheroid formation (Fig. 3B and C),

and ALDH1 positivity (Fig. 3D). Fluorogenic substrate assays indicated that SF or SO single treatment activated caspase-3/7, caspase-8, and caspase-9 only marginally, whereas the combination strongly activated caspase-3/7, caspase-8, and caspase-9 in both cell lines with an additive effect (Fig. 4A). To investigate whether SF- and SO-induced apoptosis could be abrogated by caspase inhibition, we preincubated cells with pan-caspase inhibitor Z-VAD-FMK for 4 hours before treatment (Fig. 4B). Z-VAD-FMK significantly decreased apoptosis in both cell lines as evaluated by Nicoletti staining and detection of DNA fragmentation by FACS analysis. To determine whether the expression of antiapoptotic proteins was altered, we examined cIAP-1, XIAP, and cFLIP expression by Western blot. Generally, there was a difference in basal expression of antiapoptotic proteins between the two cell lines: Whereas cIAP, XIAP, and cFLIP were highly expressed in CSC^{high} cells, only cIAP was highly expressed in CSC^{low} cells, which reflects the higher apoptosis sensitivity of this latter cell line (Fig. 4C). Correspondingly, the effects of SO and SF on expression of antiapoptotic proteins were more pronounced in CSC^{high} cells because both SF and SO reduced the expression of cIAP, XIAP, and cFLIP, whereas the effect was highest with the combination treatment. In combined therapy, SF increases targeting of CSC characteristics by SO, involving colony and spheroid formation, ALDH1 activity, and apoptosis resistance.

SF completely abolishes SO-induced NF-κB activity in CSC^{high} cells

To investigate whether SO may sensitize pancreatic CSCs by affecting NF-κB survival signaling, we performed gel retardation assays. Unexpectedly, we found a strong increase of DNA binding induced by SO in both cell lines (Fig. 5A). Although SF itself did not enhance promoter binding of NF-κB complexes, it mediated a marked reduction of SO-induced NF-κB activity in BxPc-3 CSC^{low} cells and totally abolished it in MIA-PaCa2 CSC^{high} cells. To elucidate the transactivation activity, we analyzed the composition of the SO-induced NF-κB complexes

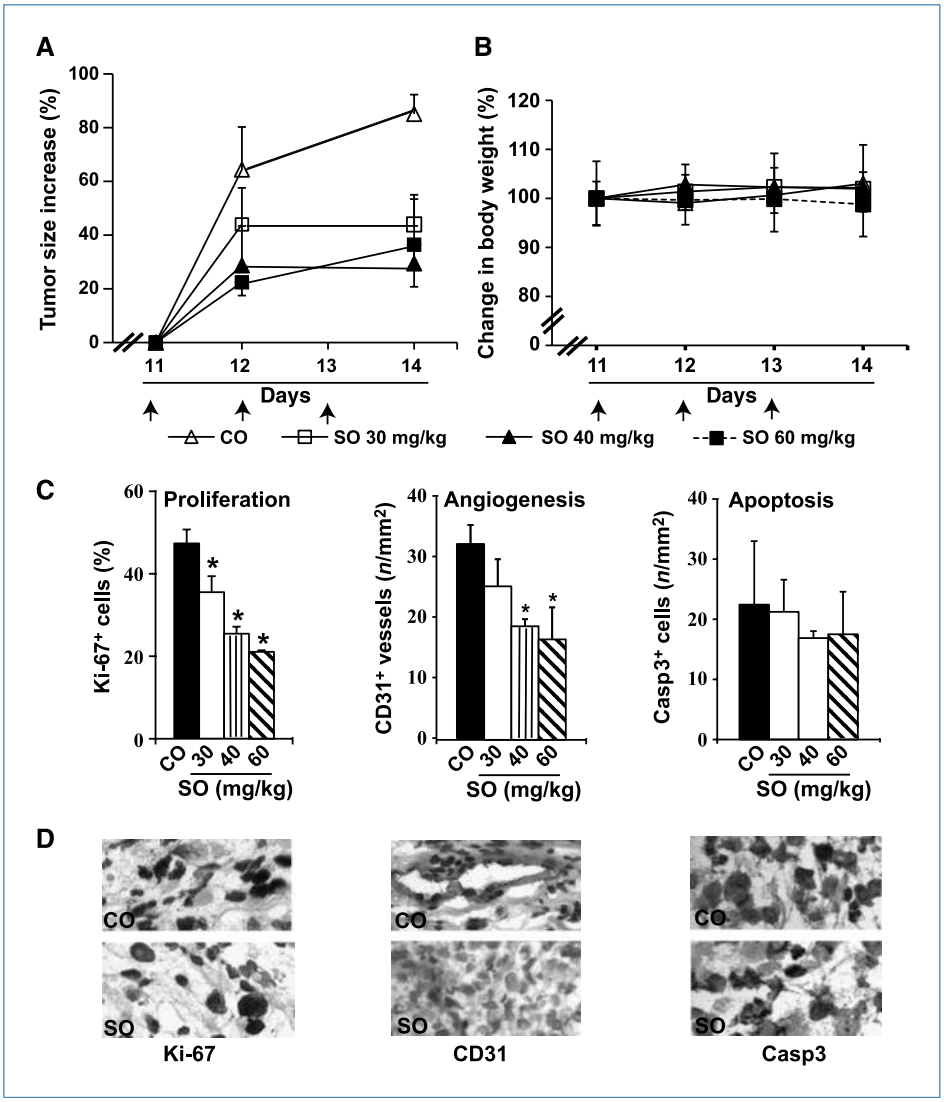

Figure 2. SO reduces xenograft tumor growth without side effects and reduces tumor proliferation and angiogenesis. A, mice were inoculated s.c. with CSC^{high} cells and treated as described in Materials and Methods. Points, mean tumor growth of three animals; bars, SD. B, the body weight of each individual mouse was set to 100% before treatment. Relative changes in the body weight after treatment with SO are shown. C, xenografts were collected 17 d after tumor cell engraftment. Frozen tumor tissue sections were subjected to immunohistochemistry for Ki-67 and CD31 (Ki-67 expression was calculated as percentage of positive tumor cells from total tumor cell mass and CD31 expression as positive vessels per square millimeter of tumor tissue in 10 vision fields under 400× magnification). Similarly, apoptosis was evaluated based on the density of active caspase-3–positive ($Casp3^+$) cells.

by incubation of cell extracts with the NF-κB consensus sequence in the presence of specific antibodies recognizing the various NF-κB subunits (Fig. 5B). In both cell lines, a selective supershift of p65 (RelA) was observed, whereas p50 and cRel could not be detected. In addition, RelB- and p52-specific shifts did not occur (data not shown). To evaluate p65 (RelA) activity by its phosphorylation pattern, we performed Western blot analysis with antibodies recognizing total p65 and phosphorylated p65. In line with the gel retardation assays, treatment with SO, but not with SF, led to a stronger phosphorylation of p65 (Fig. 5C). Combination of SO and SF slightly diminished phosphorylation of p65 in CSC^{low} cells, but not in CSC^{high} cells. These results indicate binding of a high amount of transactivation-potent p65 (RelA)-containing NF-κB dimers on treatment with SO. SF inhibits DNA binding but not the phosphorylation pattern of p65. Because NF-κB activity is associated with increased cell migration, we investigated whether SO affects the cell motility of MIA-PaCa2 CSC^{high} cells. Short-term scratch assays were performed under hypoxic conditions to enhance migratory activity. Compared with cells cultured under normoxic conditions, hypoxia led to faster migration of CSC^{high} cells into the wounded region (Fig. 5D). SF, but not SO, strongly inhibited hypoxia-induced migration. However, SO completely prevented the migratory potential on coincubation with SF.

SF and SO synergistically inhibit the growth of pancreatic CSC xenografts

To evaluate the *in vivo* effects of combined SF and SO treatment, we s.c. xenografted MIA-PaCa2 CSC^{high} cells into nude mice. After treatment, tumor size and body weight of mice were monitored daily. Treatment with SO or SF alone retarded tumor growth, but combined SF and SO treatment was strongest and significantly reduced tumor growth ($P < 0.05$; Fig. 6A). Importantly, there was neither a change in body weight of mice (Fig. 6A, right) nor a significant elevation of plasma levels of lactate dehydrogenase, aspartate aminotransferase, or alanine aminotransferase (Supplementary Fig. S2A), suggesting that the treatment was not toxic. To investigate the potential mechanisms of tumor growth retardation, tissue samples were analyzed by immunohistochemistry. Double staining of CD31 and active caspase-3–positive cells in xenograft samples indicated that tumor vascularity was reduced and apoptosis was induced on combined treatment with SO and SF

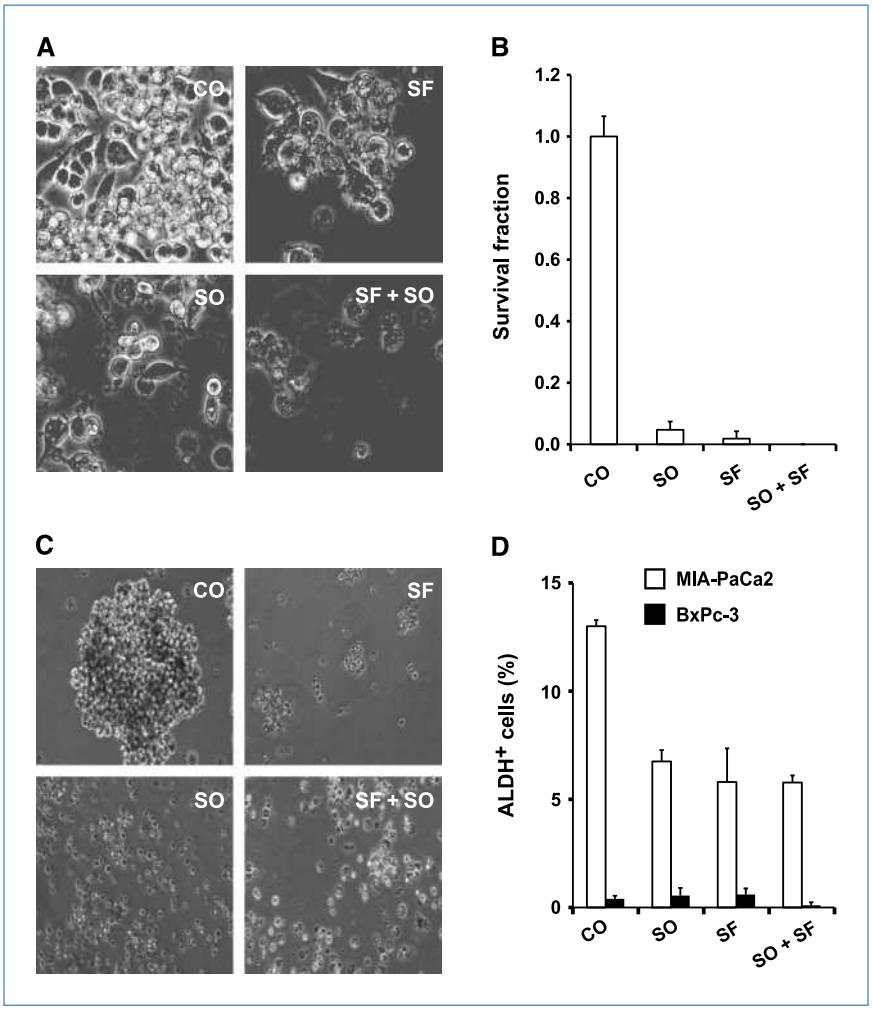

Figure 3. Combination of SF with SO enhances elimination of CSC characteristics. A, CSC^{high} cells were treated with SF (10 μmol/L, 72 h), SO (20 μmol/L, 48 h), or the two agents combined (SO + SF); representative photographs are shown (100× magnification). B, colony formation was done as described in Fig. 1B. C, spheroid formation was done as described in Fig. 1C. D, CSC^{high} and CSC^{low} cells were treated with SF, SO, or the two agents combined as described in A, and 24 h later, ALDH1 activity was analyzed by flow cytometry. The percentage of ALDH1-positive cells is presented.

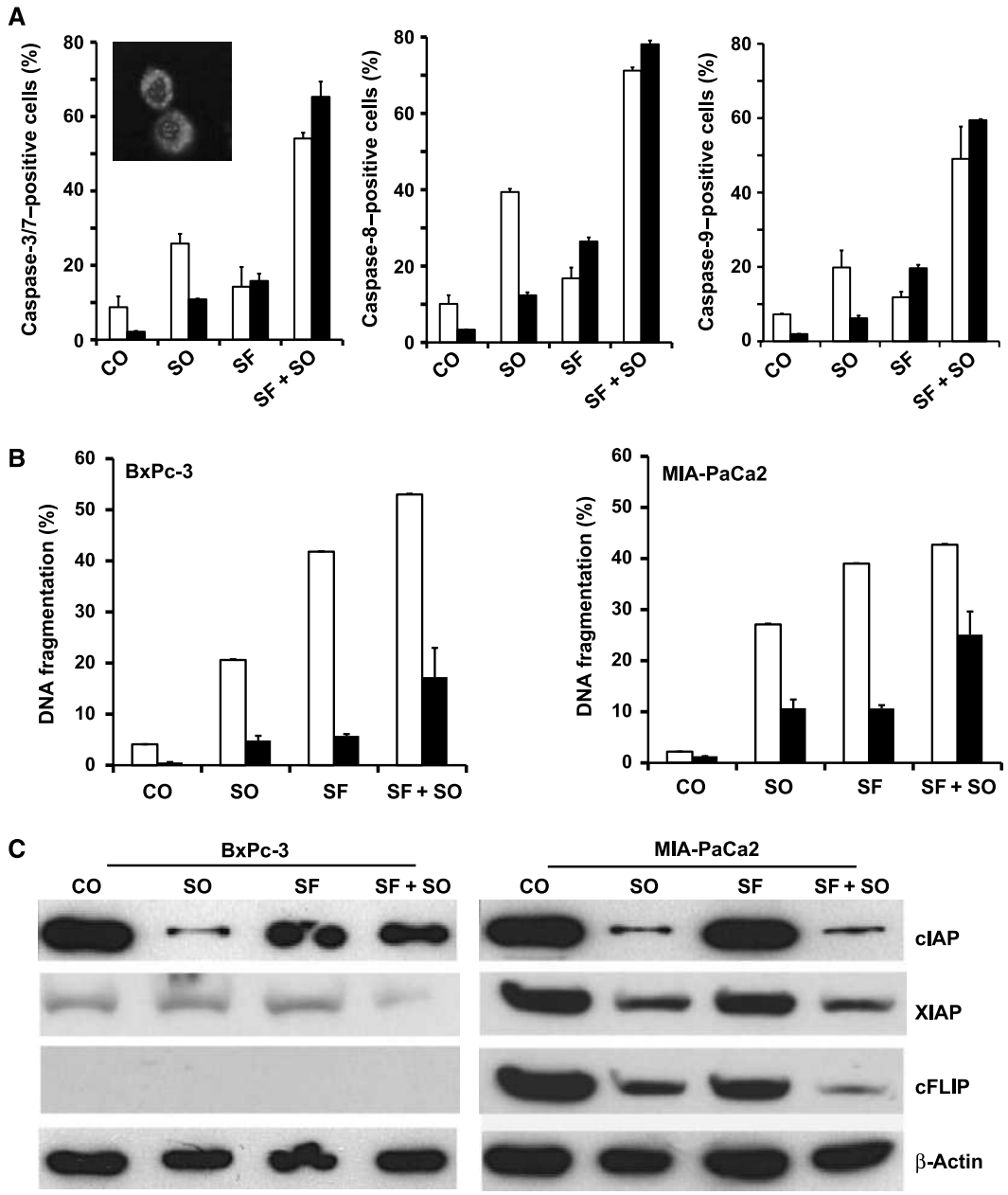

Figure 4. Combination of SF with SO overcomes apoptosis resistance of CSCs. A, CSC^{high} (white columns) and CSC^{low} (black columns) cells were treated with SF (10 μmol/L, 96 h) or SO (20 μmol/L, 72 h). Seventy-two hours later, the activity of caspase-8, caspase-9, and caspase-3/7 was measured by FLICA staining and analyzed by flow cytometry. One representative immunofluorescence image of active caspase-3/7 in CSC^{low} cells that were cotreated with SF + SO is shown. B, CSC^{low} and CSC^{high} cells were either left untreated (white columns) or preincubated with Z-VAD-FMK (40 μmol/L) for 4 h (black columns) and then exposed to SF (72 h), SO (48 h), or the two agents combined (SF + SO). Apoptosis induction was evaluated by Nicoletti staining and flow cytometry. C, twenty-four hours after treatment, expression of cIAP-1, XIAP, and cFLIP proteins was analyzed by Western blot. Expression of β-actin served as a loading control.

(Fig. 6B). Furthermore, we observed a strong reduction of tumor cell proliferation after combined SF and SO treatment as analyzed by Ki-67 immunostainings. Finally, we investigated protein expression involved in epithelial-mesenchymal transition (EMT), which has been associated with early signs of metastasis following tumor hypoxia and NF-κB activity (27, 28). First, SO, but not SF, strongly increased the expression of HIF-1α, suggesting induction of hypoxia by SO. Combination with SF decreased the induction of hypoxia by SO (Fig. 6C). Correspondingly, the EMT proteins Zeb-1 and Twist2 were

upregulated after SO treatment, whereas SF treatment alone had no effect; however, their expression decreased after cotreatment with SO and SF. Expression of vimentin, a mesenchymal cell marker, was already upregulated in untreated CSC^{high} tumors and not further affected by SO. In contrast, SF alone or in combination with SO downregulated vimentin expression. Taken together, these data suggest that growth retardation of CSC^{high} tumor xenografts by combined SF and SO treatment involves antiangiogenic, antiproliferative, and proapoptotic mechanisms. Moreover, SO-induced inhibition of angiogenesis may have been the reason for hypoxia induction, which may be, together with SO-induced NF-κB activity, the reason for the observed enhanced expression of proteins involved in EMT.

Discussion

Here, we show that the multikinase inhibitor SO alone diminishes pancreatic CSC-like tumor cells, but depletes them significantly only in combination with the phytochemical SF. The major CSC characteristics of the CSC^{high} MIA-PaCa2 and CSC^{low} BxPc-3 cell lines have been described in our recent study (6). In the present work, we describe the presence of two cell populations, which can be found in CSC^{high} but not in CSC^{low} cells, namely, spheroidal cells and fibroblast-like adherent cells. These two populations may correspond to primitive CSCs and differentiated daughter cells, suggesting differentiation potential of *in vitro* cultured pancreatic CSCs. SO targeted both cell subpopulations present in the

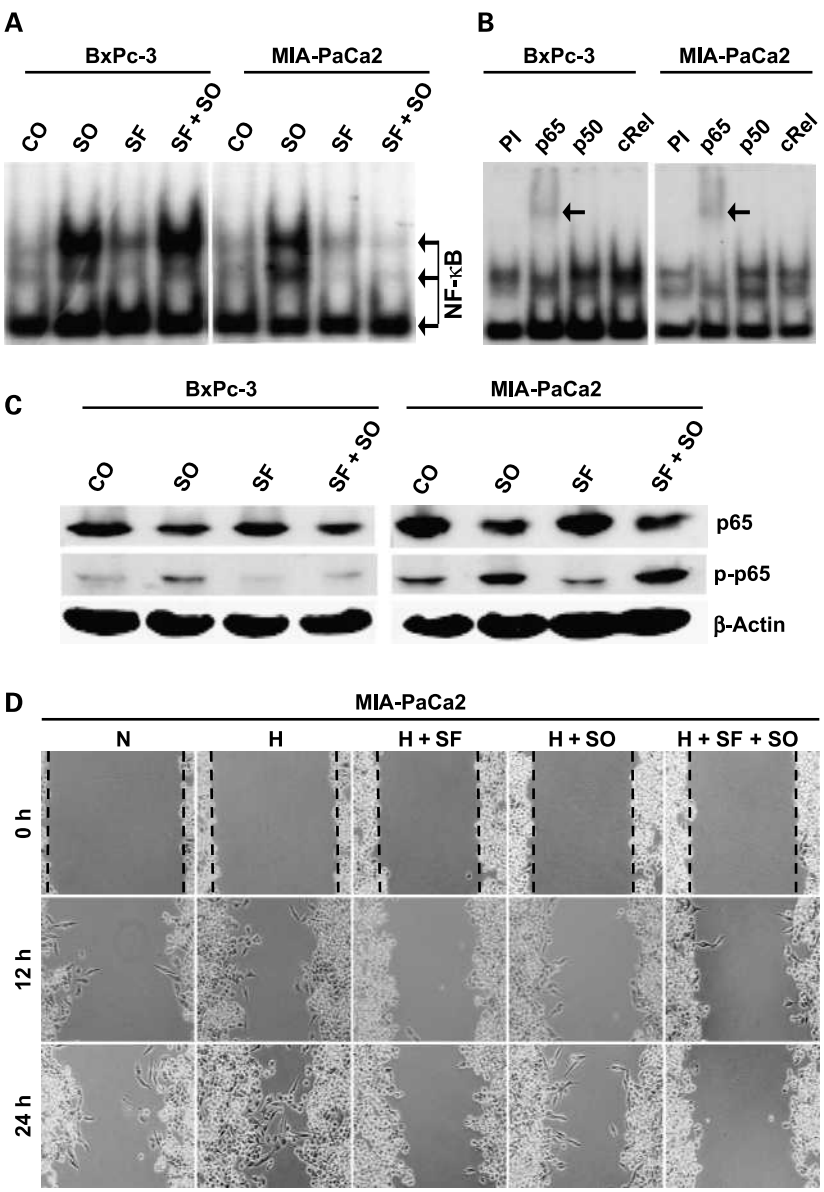

Figure 5. SF cotreatment prevents SO-mediated activation of NF-κB in CSC^{high} cells. A, whole-cell extracts were prepared 16 h after treatment and DNA binding was analyzed by EMSA using a specific ^{32}P-labeled oligonucleotide probe for NF-κB. B, nuclear proteins derived from SO-treated cells were preincubated for 30 min with specific p65, p50, or cRel antibodies for NF-κB subunits followed by EMSA analysis. Preincubation with propidium iodide served as a positive control. C, twenty-four hours after treatment, expression of whole p65 protein and phosphorylated p65 (p-p65) was analyzed by Western blot. Expression of β-actin served as a loading control. D, the effects of SF, SO, or combined SF and SO treatment on the migratory potential of CSC^{high} cells were analyzed under normoxic and hypoxic (H) conditions. Migration was analyzed 12 and 24 h after incubation and photographs were taken using a Nikon Eclipse TS100 microscope (100× magnification).

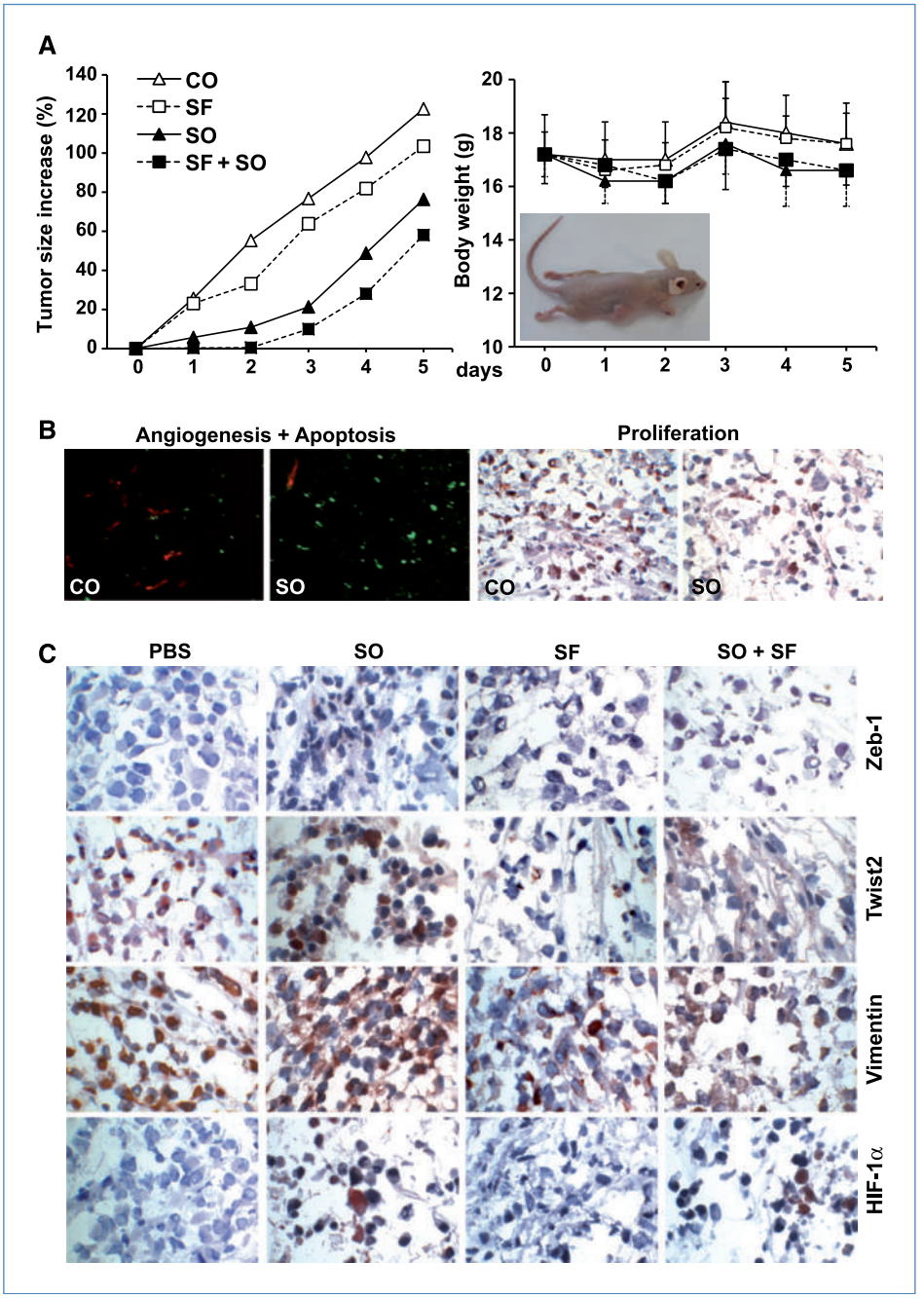

Figure 6. SF and SO cotreatment inhibits xenograft tumor growth synergistically without side effects. A, mice s.c. xenografted with CSC^{high} cells were treated and analyzed as described in Materials and Methods. Data are presented as mean of five animals. Relative changes in the mouse body weight are shown. B, frozen xenograft tumor tissue sections were subjected to double immunofluorescence staining. CD31-positive blood vessels were visualized with Alexa Fluor 594 (red) and active caspase-3–positive cells with Alexa Fluor 488 (green). Tumor cell proliferation was analyzed as described in Fig. 2D. C, frozen xenograft tumor tissue sections were analyzed by immunohistochemistry for the expression of HIF-1α and the EMT-related proteins Zeb-1, Twist2, and vimentin; representative photographs are shown under 400× magnification.

CSC^{high} cell line *in vitro*. This was due to the induction of apoptosis, DNA fragmentation, and downregulation of antiapoptotic proteins. In addition, SO strongly diminished clonogenicity, spheroid formation, and ALDH1 activity. Most importantly, the concentration of 20 μmol/L SO was selectively toxic to CSCs but not to nonmalignant primary skin fibroblasts and bone marrow–derived mesenchymal stem/stromal cells. This finding corresponds to our *in vivo* results showing that treatment of mice harboring CSC^{high} xenografts with SO reduced tumor growth in a dose-dependent manner, without obvious side effects to mice, as the general state of health, body weight, and liver parameters were constant during and after treatment. Reduction of pancreatic tumor xenografts was due to inhibition of proliferation and angiogenesis and induction of apoptosis. Our results confirm data obtained in thyroid carcinoma and hepatocellular carcinoma xenograft models (29, 30), in which the authors describe inhibition of angiogenesis and tumor growth along with induction of apoptosis following treatment of the mice with SO.

We are the first to report increased NF-κB activity on SO treatment. We found induction of p65 (RelA)-containing transactivation-competent dimers by SO as shown by

supershift assays and detection of phosphorylated p65 proteins by Western blot analysis. This result was surprising because NF-κB activity may render tumor cells resistant to conventional cancer therapy. However, many chemotherapeutic agents and the apoptosis-inducing ligand tumor necrosis factor–related apoptosis-inducing ligand share this unwanted feature of SO and can activate NF-κB (6). Basal NF-κB overexpression is observed in various malignant tumors including pancreatic adenocarcinoma and has been made responsible for high therapy resistance of pancreatic tumor cells (31, 32). We assume that enhanced NF-κB binding by SO could be the reason for the observed selection of resistant CSC^{high} clones on long-term treatment with SO. NF-κB was recently identified as a central mediator of EMT and metastasis in a model of breast cancer (28). Our xenograft studies suggest that NF-κB activity may be involved in induction of EMT following SO treatment, resulting in the selection of a more invasive and metastatic phenotype. Such a scenario has recently been described, as transcription factors involved in EMT are possible downstream targets of NF-κB (33, 34).

To overcome SO-induced NF-κB activity and associated resistance, we chose SF for cotreatment because we recently showed that this broccoli-derived isothiocyanate is able to sensitize pancreatic CSCs toward conventional therapy by strong downregulation of NF-κB activity (6). Indeed, SF totally abolished SO-induced NF-κB binding in CSC^{high} cells, whereas no effect in CSC^{low} cells was observed. SF may directly interfere with promoter binding of p65 (RelA), rather than downregulating p65 phosphorylation, as we conclude from our supershift assays and Western blot analysis of phosphorylated p65. Furthermore, combination of SO with SF considerably reduced the clonogenicity and self-renewal potential of CSCs and enhanced apoptosis *in vitro*. In addition, suppression of NF-κB sensitized CSCs to SO-induced apoptosis, as measured by caspase activity and DNA fragmentation. Although we were not able to detect any NF-κB changes in xenografts, this transcription factor may be involved in the observed effects in tumors because several *in vivo* studies show that blocking of NF-κB in pancreatic cancer affects angiogenesis, apoptosis, and proliferation (35).

A notable recent observation by other authors is that SO and related antiangiogenic substances induce pronounced initial tumor growth retardation. However, this is followed by adaptation of the tumor to treatment and subsequent regrowth (18, 19). Our results confirm this observation because a few clones of our long-term treated CSC^{high} cells adapted to SO treatment and survived. These results match our *in vivo* findings, where inhibition of angiogenesis by SO may have induced hypoxia and EMT. Another potential mechanism explaining the tumor regrowth in the presence of SO could be that after transient vessel reduction induced by the antiangiogenic treatment, the delivery of therapeutic substances is impaired.

In conclusion, our data show that although SO is initially effective, it does not lead to total elimination of CSCs, which start to regrow after an interim. Combination with an NF-κB inhibitor such as SF may be a therapeutic option to improve the therapeutic effect of SO.

Disclosure of Potential Conflicts of Interest

No potential conflicts of interest were disclosed.

Acknowledgments

We thank Bayer Corporation for sorafenib and H-J. Stark for primary skin fibroblasts.

Grant Support

Bundesministerium für Bildung und Forschung (01GU0611), Tumorzentrum Heidelberg/Mannheim (D10027(6)350), Stiftung Chirurgie Heidelberg, Dietmar-Hopp Stiftung, Deutsche Krebshilfe (107254), and Deutsche Forschungsgemeinschaft (SFB 518/A17).

The costs of publication of this article were defrayed in part by the payment of page charges. This article must therefore be hereby marked *advertisement* in accordance with 18 U.S.C. Section 1734 solely to indicate this fact.

Received 01/19/2010; revised 03/26/2010; accepted 04/08/2010; published OnlineFirst 06/08/2010.

References

1. Gukovskaya AS, Pandol SJ. Cell death pathways in pancreatitis and pancreatic cancer. Pancreatology 2004;4:567–86.
2. Olempska M, Eisenach PA, Ammerpohl O, Ungefroren H, Fandrich F, Kalthoff H. Detection of tumor stem cell markers in pancreatic carcinoma cell lines. Hepatobiliary Pancreat Dis Int 2007;6:92–7.
3. Li C, Heidt DG, Dalerba P, et al. Identification of pancreatic cancer stem cells. Cancer Res 2007;67:1030–7.
4. Hermann PC, Huber SL, Herrler T, et al. Distinct populations of cancer stem cells determine tumor growth and metastatic activity in human pancreatic cancer. Cell Stem Cell 2007;1:313–23.
5. Zhou BB, Zhang H, Damelin M, Geles KG, Grindley JC, Dirks PB. Tumour-initiating cells: challenges and opportunities for anticancer drug discovery. Nat Rev Drug Discov 2009;8:806–23.
6. Kallifatidis G, Rausch V, Baumann B, et al. Sulforaphane targets pancreatic tumour-initiating cells by NF-κB-induced antiapoptotic signalling. Gut 2009;58:949–63.
7. Mimeault M, Hauke R, Mehta PP, Batra SK. Recent advances in cancer stem/progenitor cell research: therapeutic implications for overcoming resistance to the most aggressive cancers. J Cell Mol Med 2007;11:981–1011.
8. Jones RJ, Matsui WH, Smith BD. Cancer stem cells: are we missing the target? J Natl Cancer Inst 2004;96:583–5.
9. Kupsch P, Henning BF, Passarge K, et al. Results of a phase I trial of sorafenib (BAY 43-9006) in combination with oxaliplatin in patients with refractory solid tumors, including colorectal cancer. Clin Colorectal Cancer 2005;5:188–96.
10. Figer A, Moscovici M, Bulconic S, et al. Phase I trial of BAY 43-9006 in combination with 5-fluorouracil (5-FU) and leucovorin (LCV) in patients with advanced refractory solid tumors. Ann Oncol 2004;15:iii87.
11. Siu LL, Awada A, Takimoto CH, et al. A phase I/II trial of BAY 43-9006 and gemcitabine in advanced solid tumors and in advanced pancreatic cancer. J Clin Oncol ASCO Annual Meeting Proceedings 2004;22(14S):abstract 3059.
12. Richly H, Henning BF, Kupsch P, et al. Results of a phase I trial of sorafenib (BAY 43-9006) in combination with doxorubicin in patients with refractory solid tumors. Ann Oncol 2006;17:866–73.
13. Awada A, Hendlisz A, Gil T, et al. A phase I study of BAY 43-9006, a novel Raf kinase and VEGFR inhibitor, in combination with Taxotere in patients with advanced solid tumor. Eur J Cancer Suppl 2004;2:1114.

14. Flaherty KT, Brose M, Schuchter L, et al. Phase I/II trial of BAY 43-9006, carboplatin (C) and paclitaxel (P) demonstrates preliminary antitumor activity in the expansion cohort of patients with metastatic melanoma [abstract]. J Clin Oncol 2004;22:7507.
15. Vroling L, Lind JS, de Haas RR, et al. CD133$^+$ circulating haematopoietic progenitor cells predict for response to sorafenib plus erlotinib in non-small cell lung cancer patients. Br J Cancer 2010;102:268–75.
16. Wilhelm SM, Carter C, Tang L, et al. BAY 43-9006 exhibits broad spectrum oral antitumor activity and targets the RAF/MEK/ERK pathway and receptor tyrosine kinases involved in tumor progression and angiogenesis. Cancer Res 2004;64:7099–109.
17. Carlomagno F, Anaganti S, Guida T, et al. BAY 43-9006 inhibition of oncogenic RET mutants. J Natl Cancer Inst 2006;98:326–34.
18. Paez-Ribes M, Allen E, Hudock J, et al. Antiangiogenic therapy elicits malignant progression of tumors to increased local invasion and distant metastasis. Cancer Cell 2009;15:220–31.
19. Ebos JM, Lee CR, Cruz-Munoz W, Bjarnason GA, Christensen JG, Kerbel RS. Accelerated metastasis after short-term treatment with a potent inhibitor of tumor angiogenesis. Cancer Cell 2009;15:232–9.
20. Herr I, Buchler MW. Dietary constituents of broccoli and other cruciferous vegetables: implications for prevention and therapy of cancer. Cancer Treat Rev 2010 Feb 19. [Epub ahead of print].
21. Beckermann BM, Kallifatidis G, Groth A, et al. VEGF expression by mesenchymal stem cells contributes to angiogenesis in pancreatic carcinoma. Br J Cancer 2008;99:622–31.
22. Zhang C, Kolb A, Buchler P, et al. Corticosteroid co-treatment induces resistance to chemotherapy in surgical resections, xenografts and established cell lines of pancreatic cancer. BMC Cancer 2006;6:61.
23. Apel A, Herr I, Schwarz H, Rodemann HP, Mayer A. Blocked autophagy sensitizes resistant carcinoma cells to radiation therapy. Cancer Res 2008;68:1485–94.
24. Maier HJ, Marienfeld R, Wirth T, Baumann B. Critical role of RelB serine 368 for dimerization and p100 stabilization. J Biol Chem 2003;278:39242–50.
25. Koziol JA, Maxwell DA, Fukushima M, Colmerauer ME, Pilch YH. A distribution-free test for tumor growth curve analyses with application to an animal tumor immunotherapy experiment. Biometrics 1981;37:383–90.
26. Kallifatidis G, Beckermann BM, Groth A, et al. Improved lentiviral transduction of human mesenchymal stem cells for therapeutic intervention in pancreatic cancer. Cancer Gene Ther 2008;15:231–40.
27. Hill RP, Marie-Egyptienne DT, Hedley DW. Cancer stem cells, hypoxia and metastasis. Semin Radiat Oncol 2009;19:106–11.
28. Huber MA, Azoitei N, Baumann B, et al. NF-κB is essential for epithelial-mesenchymal transition and metastasis in a model of breast cancer progression. J Clin Invest 2004;114:569–81.
29. Liu L, Cao Y, Chen C, et al. Sorafenib blocks the RAF/MEK/ERK pathway, inhibits tumor angiogenesis, and induces tumor cell apoptosis in hepatocellular carcinoma model PLC/PRF/5. Cancer Res 2006;66:11851–8.
30. Kim S, Yazici YD, Calzada G, et al. Sorafenib inhibits the angiogenesis and growth of orthotopic anaplastic thyroid carcinoma xenografts in nude mice. Mol Cancer Ther 2007;6:1785–92.
31. Chandler NM, Canete JJ, Callery MP. Increased expression of NF-κ B subunits in human pancreatic cancer cells. J Surg Res 2004;118:9–14.
32. Arlt A, Gehrz A, Muerkoster S, et al. Role of NF-κB and Akt/PI3K in the resistance of pancreatic carcinoma cell lines against gemcitabine-induced cell death. Oncogene 2003;22:3243–51.
33. Kang Y, Massague J. Epithelial-mesenchymal transitions: twist in development and metastasis. Cell 2004;118:277–9.
34. Chua HL, Bhat-Nakshatri P, Clare SE, Morimiya A, Badve S, Nakshatri H. NF-κB represses E-cadherin expression and enhances epithelial to mesenchymal transition of mammary epithelial cells: potential involvement of ZEB-1 and ZEB-2. Oncogene 2007;26:711–24.
35. Xiong HQ, Abbruzzese JL, Lin E, Wang L, Zheng L, Xie K. NF-κB activity blockade impairs the angiogenic potential of human pancreatic cancer cells. Int J Cancer 2004;108:181–8.